Dual-band fractal antenna with concentric ring-shaped defected ground plane structure

Edwin Kimani Miring'u*, Kibet Langat and D. B. O. Konditi

***Abstract*—** This paper proposes the design of improved dual-band micro-strip antennas through the use of concentric rectangular fractals in the patch, and a ground plane with a concentric ring-shaped defected ground plane structure, located at the bottom of the same antenna. This design technique constitutes the fractal antenna with concentric ring-shaped defected ground plane structure. The design will be undertaken in two successive iterations. The antennas proposed in this paper have dual-band resonances at 1.7375 GHz and 2.0375 GHz for the 1st iteration, and 1.7625 GHz and 2.075 GHz for the 2nd iteration, with -10 dB impedance bandwidths of 72.5 MHz and 65.5 MHz for the 1st iteration, and 58.8 MHz and 66.8 MHz for the 2nd iteration. The designed antennas can be used for telecommunication and satellite applications.

***Keywords*—** Defected, fractal, micro-strip, multi-band.

I. INTRODUCTION

Due to the proliferation of wireless communication systems, micro-strip antennas have found increased use in these systems due to their inherent advantages such as light weight, ease off fabrication, low cost and conformability to mounting surfaces [1].

Micro-strip antennas are however faced by the disadvantage of only radiating efficiently over a narrow band of frequencies, which in turn limits the band of frequencies over which they can operate satisfactorily. The rapid development of modern mobile and wireless communication systems has thus necessitated the design of micro-strip antennas with multiband capability [2].

Various design techniques have been employed by various authors to achieve multi-band operation such as defected ground plane structure (DGPS) and use of fractal geometries in patches.

A DGPS is a simply a defect or defects excoriated in the ground plane of the antenna. The DGPSs are easy to design and implement. They are however not very complex in shape to prevent difficulty during the optimization process when particular design goals are required [3]-[9].

Fractal antennas, on the other hand, are recursively generated geometries based on the concept of a fractal. They are generated through an iterative process which leads to self-similar structures. Fractals exist in nature and can be used to model complex phenomena such as mountains, trees, clouds etc [10]. Various fractal design techniques have been carried out to improve the performance of micro-strip antennas [11]-[19].

This paper proposes the design of improved dual-band micro-strip antennas through excoriating concentric rectangular fractals in the patch and a ground plane with a concentric ring-shaped defected ground plane structure at the bottom of the same antenna. The substrate has a relative permittivity $\varepsilon_r = 4.7$ and a thickness, h of 1.6 mm.

In a previous study [20], a fractal antenna was designed, which exhibited single band resonance. This paper proposes to incorporate concentric rectangular fractals in the patch, in addition to concentric ring-shaped defects in the ground plane of the same antenna, which constitutes the fractal antenna with concentric ring-shaped defected ground plane structure (FACRDGPS). The design will be undertaken in two successive iterations (1st and 2nd).

The antennas proposed in this paper exhibit dual-band resonance at 1.7375 GHz and 2.0375 GHz for the 1st iteration, and 1.7625 GHz and 2.075 GHz for the 2nd iteration, with -10 dB impedance bandwidths of 72.5 MHz and 65.5 MHz for the 1st iteration, and 58.8 MHz and 66.8 MHz for the 2nd iteration.

The designed antennas can be used for mobile communication and satellite radio applications which require multi-band antenna for their applications and since the resonance frequencies fall in the Ultra High Frequency (UHF) band (0.3-3GHz).

II. ANTENNA DESIGN

A. Conventional inset-fed rectangular patch design

In the design of the Fractal antenna with Concentric Ring-shaped Defected ground plane Structure (FACRDGPS), a conventional rectangular micro-strip antenna is initially designed. A resonance frequency of 2.45 GHz is chosen because of its location in the Industrial, Scientific and Medical (ISM) band and also due to its low attenuation through the atmosphere.

The substrate used is FR4 with a dielectric constant ε_r of 4.7, a loss tangent of 0.02 and a thickness h of 1.6 mm. FR4 is chosen for the design due to its low cost.

A micro-strip feed line is used as the feeding technique because it is simple to match, easy to fabricate and simple to model [21]. An inset feed is used to match the patch antenna's

Edwin Kimani Miring'u, Department of Telecommunication and Information Engineering, JKUAT (corresponding author to provide phone: +254 727177541; e-mail: miringu4edwin@gail.com).

author@eng. jkuat.ac.ke).

input impedance to that of the micro-strip line (50 Ω). The conventional rectangular patch is shown in Fig.1.

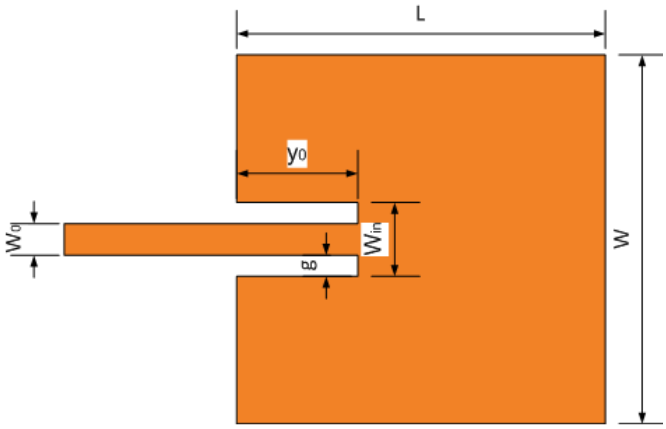

Fig. 1 An inset fed conventional rectangular patch antenna

The width W of the antenna in Fig. 1 is computed using equation (1) [1];

$$W = \frac{c}{2f_r}\left[\frac{\varepsilon_r+1}{2}\right]^{-0.5} \quad (1)$$

where c is the speed of light in m/s, f_r is the resonance frequency in Hz, and ε_r is the dielectric constant.

The effective dielectric constant, ε_{reff} is then computed using equation (2) [1];

$$\varepsilon_{reff} = \frac{\varepsilon_r+1}{2} + \frac{\varepsilon_r-1}{2}\left[1+\frac{12h}{W}\right]^{-0.5} \quad (2)$$

where h is the height/thickness of the substrate in m.

The extension of the length, ΔL due to fringing of electric fields is then computed using equation (3) [1];

$$\Delta L = 0.412h\frac{[\varepsilon_{reff}+0.3]}{[\varepsilon_{reff}-0.258]}\frac{\left[\frac{W}{h}+0.264\right]}{\left[\frac{W}{h}+0.8\right]} \quad (3)$$

The effective length of the patch L_{eff} is then computed using equation (4) [1];

$$L_{eff} = \frac{c}{2f_r\sqrt{\varepsilon_{reff}}} \quad (4)$$

The actual length of the patch L is then computed using equation (5) [1];

$$L = L_{eff} - 2\Delta L \quad (5)$$

The ground plane length L_g and width W_g are then computed using equation (6) and (7) respectively [1];

$$L_g = L + 12h \quad (6)$$

$$W_g = W + 12h \quad (7)$$

The characteristic impedance Z_c of the micro-strip line feed is given by equation (8). From equation (8), the width of the micro-strip line feed is computed [1].

$$Z_c = \frac{120\pi}{\sqrt{\varepsilon_{reff}}}\left[\frac{W_0}{h} + 1.393 + 0.667\ln\left(\frac{W_0}{h}+1.444\right)\right] \quad (8)$$

where W_0 is the width of the micro-strip line feed in m. Since equation (8), doesn't have a closed form solution, a MATLAB code was used to compute W_0.

The inset width W_{in} as shown in Fig.1, is calculated using equation (9) [22];

$$W_{in} = \frac{W}{5} \quad (9)$$

The gap g of the inset feed is then calculated using equation (10) [22];

$$g = \frac{W_{in}-W_0}{2} \quad (10)$$

The input resistance R_{in} for the inset feed is given by equation (11) [1];

$$R_{in}(y = y_0) = R_{in}(y = 0)\cos^2\frac{\pi}{L}y_0 \quad (11)$$

where y_0 is the inset feed distance in m. A MATLAB code was used to compute the input resistance at the leading radiating edge of the antenna. The same MATLAB code was also used to compute the inset feed distance y_0.

After the initial design computations, the antenna design and simulation are carried out using High Frequency Structure Simulator (HFSS) simulation software. Optimization of the patch length L and width W is done for resonance at exactly 2.45 GHz. The optimized patch length and width dimensions are denoted by L_{opt} and W_{opt}, respectively in Table I.

The computed parameters of the inset fed-rectangular patch antenna are indicated in Table I.

Table I Dimensions of the conventional inset-fed rectangular patch

Antenna Parameter	Notation	Dimension
Calculated patch	$L \times W$	27.91×36.27
Optimized patch	$L_{opt} \times W_{opt}$	28 × 34
Ground plane	$L_g \times W_g$	47.10×55.47
Substrate	$L_s \times W_s$	47.10×55.47
Inset feed distance	y_0	10.42
Micro-strip line width	W_0	3.2
Notch width	g	2.03

B. Fractal antenna with concentric ring-shaped defected ground plane structure (FACRDGPS) design

In designing the Fractal Antennas with Concentric Ring-shaped DGPS (FACRDGPS), a defected ground plane structure

(DGPS) based on concentric rings was incorporated in the ground plane, in the 1st and 2nd iterations of a Fractal antenna. Thus the 1st iteration FACRDGPS is designed and subsequently, the 2nd iteration FACRDGPS is designed.

i. 1st iteration FACRDGPS Design

The 1st iteration FACRDGPS incorporates a 1st iteration fractal in the patch of the antenna and a concentric ring shaped DGPS in the ground plane of the antenna.

The 1st iteration Fractal antenna is shown in Fig. 2. For the 1st iteration fractal, two concentric rectangles are used in generating the fractal. The main patch is divided into 9 rectangles each of dimensions $L_{01} \times W_{01}$. L_{01} is $\frac{1}{3}$ of L whereas W_{01} is $\frac{1}{3}$ of W.

Another rectangle with the dimensions $L_{i1} \times W_{i1}$ is designed. L_{i1} is $\frac{1}{4}$ of L whereas W_{i1} is $\frac{1}{4}$ of W. The subscripts 0 and i imply the outer and inner rectangle, respectively. The subscript 1 implies the 1st iteration. Thus the outer rectangle has the dimensions $L_{01} \times W_{01}$ being equal to 9.3333×11.3333 mm^2, whereas the inner rectangle has the dimensions $L_{i1} \times W_{i1}$ being equal to 7×8.5 mm^2.

Using the two concentric rectangles of dimensions $L_{01} \times W_{01}$ at the center of the patch, which is the central rectangle of the 9 rectangles that the patch was sub-divided into, Boolean subtraction is carried out using the HFSS simulation software. This gives rise to the concentric fractal rectangle as depicted in Fig. 2. This constitutes the 1st iteration fractal antenna shown in Fig. 2.

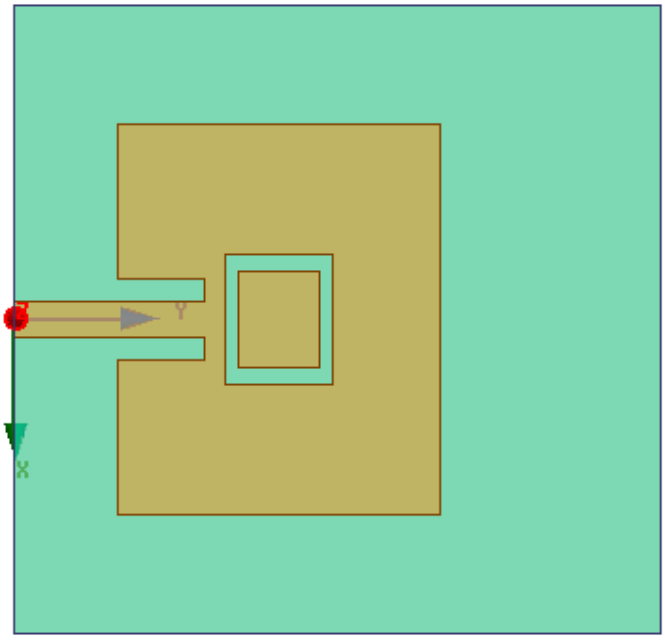

Fig. 2 1st iteration fractal antenna

The concentric ring-shaped defected ground plane structure (CRDGPS), based on concentric circles, is excoriated in the ground plane of the antenna to form the concentric ring-shaped defected ground plane structure micro-strip antenna (CRDGPSMA). The dimensions of the CRDGPS are indicated in Table II. The CRDGPSMA is depicted in Fig. 3.

Table II Dimensions of the concentric ring-shaped defected ground plane structure (CRDGPS)

Dimensions of the CRDGPS (mm)							
R_1	R_2	R_3	R_4	R_5	R_6	R_7	R_8
8.5	7	11.5	10	14.5	13	17.5	16

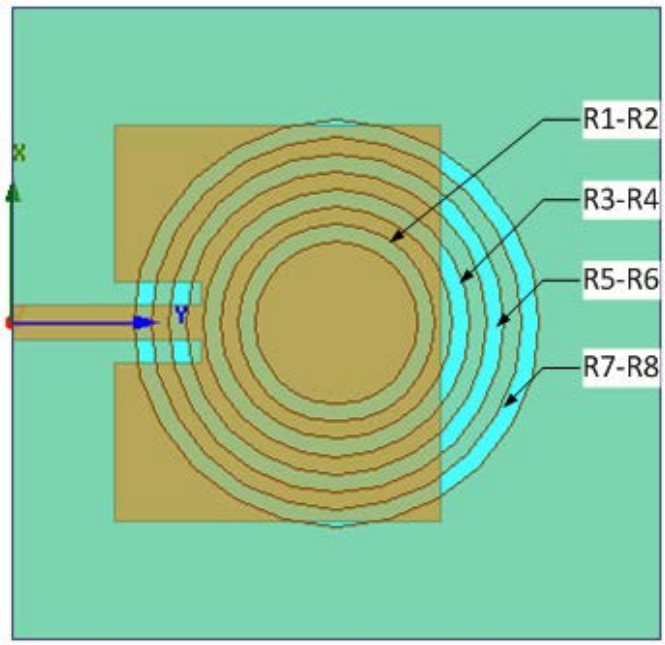

Fig. 3 The concentric ring shaped defected ground plane structure incorporated in the ground plane of the antenna

By incorporating both design techniques in the same antenna as detailed above; the 1st iteration fractal in the patch of the antenna and excoriating the concentric ring-shaped defected ground plane structure in the ground plane, a 1st iteration fractal antenna with concentric ring-shaped defected ground plane structure (1st iteration FACRDGPS) is designed. The 1st iteration FACRDGPS is depicted in Fig. 4.

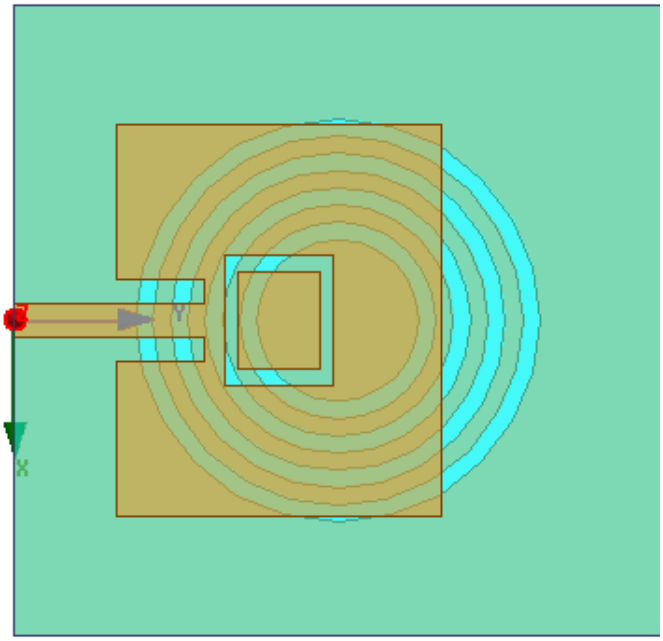

Fig. 4 1st iteration Fractal antenna with Concentric Ring-shaped DGPS (1st iteration FACRDGPS)

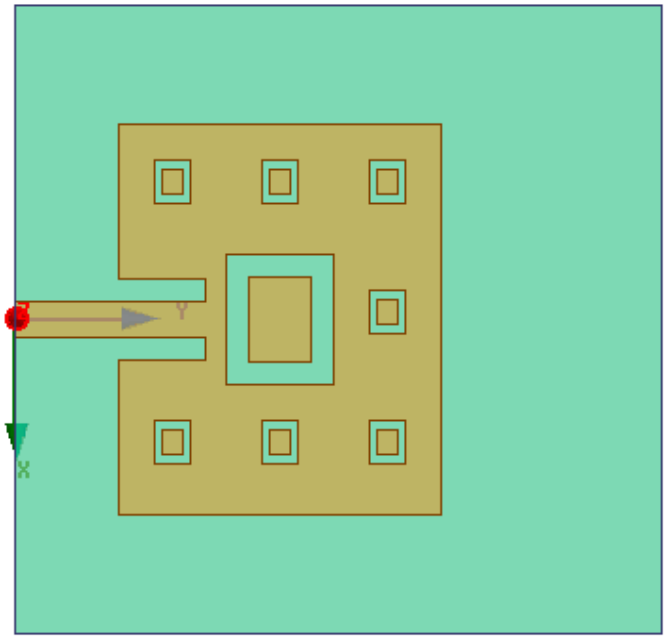

Fig. 5 The 2nd iteration fractal antenna

ii. 2nd iteration FACRDGPS

In designing the 2nd iteration Fractal antenna, the 1st iteration fractal antenna designed in the section above and shown in Fig. 2 is used.

Each of the 9 rectangles into which the main patch was initially sub-divided, is further sub-divided into 9 rectangles. The dimensions of each of these small rectangles are $L_{02} \times W_{02}$. L_{02} is $\frac{1}{3} L_{01}$ whereas W_{02} is $\frac{1}{3} W_{01}$.

An additional rectangle is created with the dimensions $L_{i2} \times W_{i2}$. L_{i2} is $\frac{1}{4} L_{i2}$ whereas W_{i2} is $\frac{1}{4} W_{i1}$. The subscripts o and i imply the outer and inner rectangle, respectively. The subscript 2 denotes the 2nd iteration.

Thus, the outer rectangle had the dimensions $L_{02} \times W_{02}$ equal to 3.1111×3.7778 mm^2, whereas the inner rectangle had the dimensions $L_{i2} \times W_{i2}$ equal to 1.75×2.125 mm^2.

Using the two concentric rectangles of dimensions $L_{02} \times W_{02}$ and $L_{i2} \times W_{i2}$ at the center of each of the 9 sub-rectangles that each of the 9 rectangles in the 1st iteration fractal is subdivided into, Boolean subtraction is carried out using the HFSS simulation software, to form 7 smaller concentric fractal rectangles. One set of concentric fractal rectangle couldn't be excoriated due to the location of the micro-strip feed line. This gives rise to the fractal concentric rectangles as depicted in Fig. 5. This constituted the 2nd iteration fractal antenna, shown in Fig. 5.

The 2nd iteration fractal antenna with concentric ring-shaped defected ground plane structure (FACRDGPS) design involves excoriating 2nd iteration fractals in the patch and concentric ring-shaped defects in the ground plane of the antenna. The concentric ring-shaped defected ground plane structure to be used is the same as the one depicted in Fig. 3. Combining these two design techniques results in a 2nd iteration FACRDGPS. The 2nd iteration FACRDGPS is illustrated in Fig. 6.

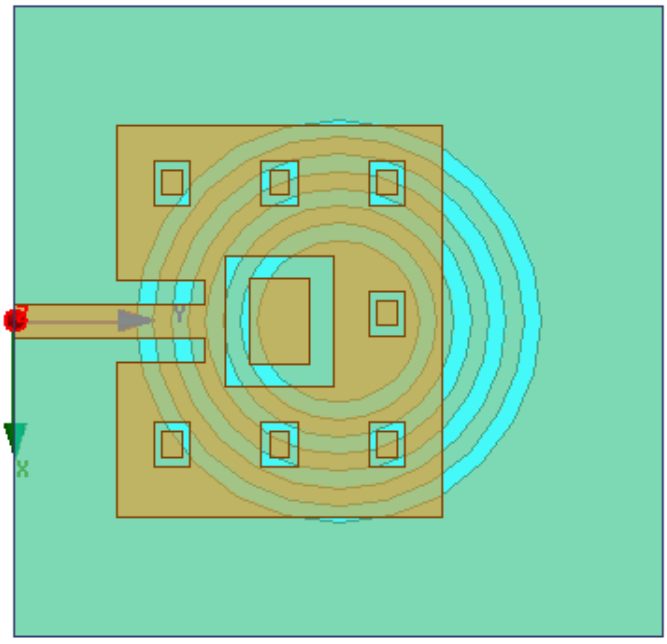

Fig. 6 2nd iteration fractal antenna with concentric ring-shaped defected ground plane structure (FACRDGPS)

III. RESULTS AND DISCUSSION

A. Conventional inset fed rectangular patch

The return loss plot of the conventional inset fed rectangular patch is shown in Fig. 7. For good power coupling, the return loss should be less than -10 dB. The return loss for the conventional inset fed rectangular patch is -21.5064 dB at a resonance frequency of 2.45 GHz with -10 dB impedance bandwidth was 67.5 MHz.

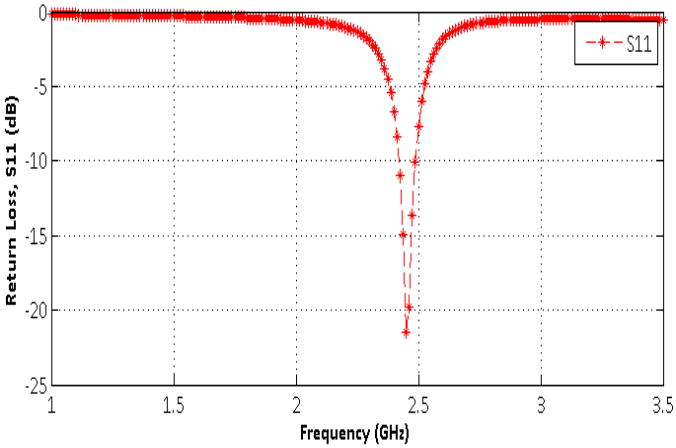

Fig. 7 Return loss plot of the conventional inset fed rectangular patch.

The Voltage Standing Wave Ratio (VSWR) plot is depicted in Fig. 8. Across the band from 2.4190 GHz--2.4896 GHz, the VSWR is observed to be < 2. This is indicative of good impedance matching which prevents power from being reflected back to the source, which would lead to power losses.

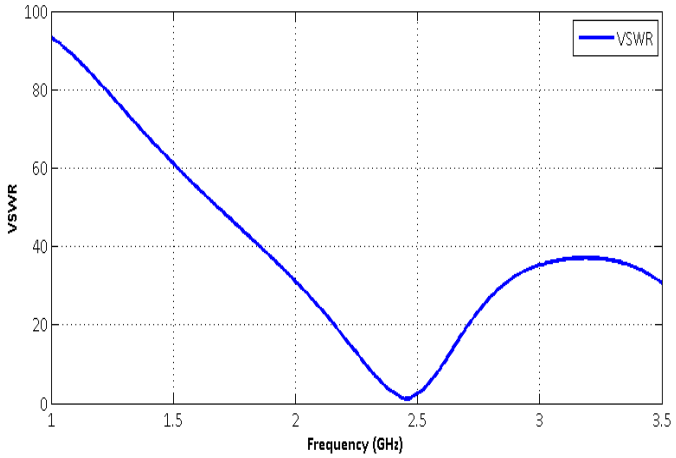

Fig. 8 VSWR plot of the conventional inset fed patch antenna

In order to study the excitation mechanism of the conventional inset fed rectangular patch, the current distribution of the antenna is studied. This is shown in Fig. 9. Fig. 9(a) shows the magnitude form of the current distribution whereas Fig. 9(b) shows the current distribution in vector form. The current distribution is observed to be concentrated along the mid-section of the antenna. This can be attributed to the fact that most of the radiation occurs from this section.

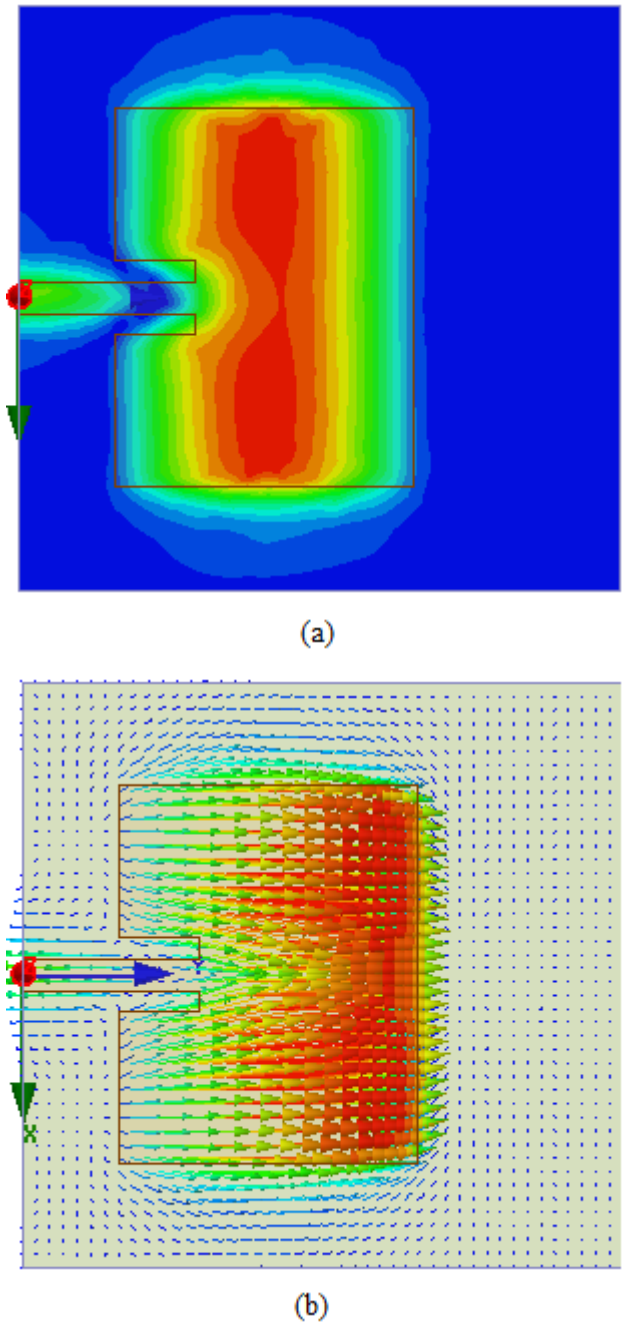

Fig. 9 Current distribution of the conventional patch antenna at 2.45 GHz; (a) Magnitude form (b) Vector form

From the current distribution plot (in vector form) of the conventional patch antenna shown in Fig. 9(b), it is observed that current flows in the *y*-direction. Thus, the *yz*-plane is the *E*-plane whereas the *xz*-plane is the *H*-plane. The radiation patterns for the conventional patch antenna in the *E*-plane and the *H*-plane at 2.45 GHz are plotted in Fig. 10.

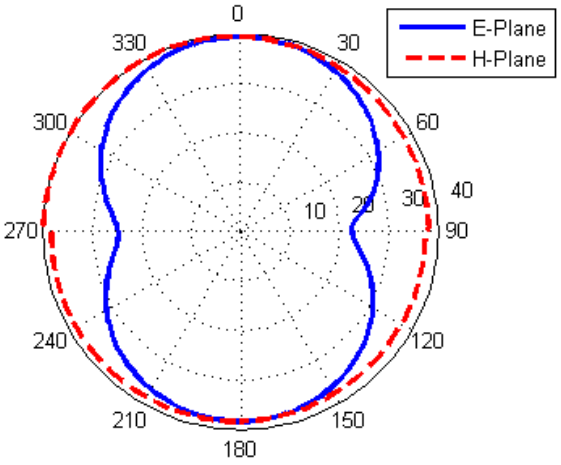

Fig. 10 Radiation pattern of the conventional patch antenna at 2.45 GHz

The radiation pattern in the *E*-plane is observed to be bi-directional whereas the one in the *H*-plane was observed to be omni-directional. The radiation patterns are observed to be symmetrical due to the symmetrical structure of the conventional patch antenna.

B. 1st iteration FACRDGPS Design

The return loss plots of the 1st iteration Fractal antenna with concentric ring-shaped DGPS (FACRDGPS) are shown in Fig. 11. The return loss plots of the Concentric Ring-shaped DGPSMA and fractal iteration 1 antenna are included for comparison.

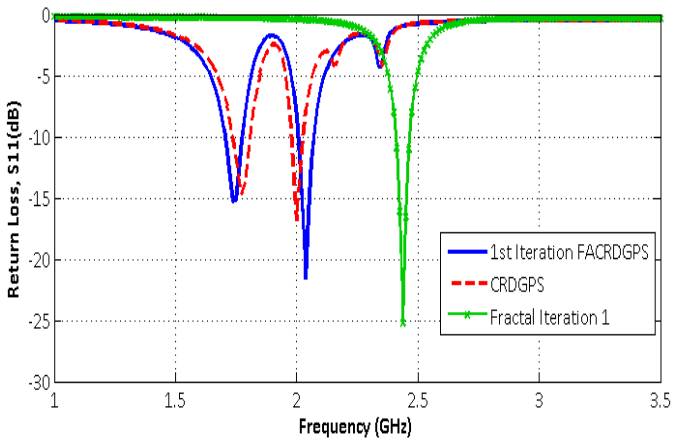

Fig. 11 Combined return loss plot of the 1st iteration FACRDGPS, Concentric Ring-shaped DGPSMA and the 1st iteration Fractal antenna

The 1st iteration FACRDGPS exhibits dual-band resonance, resonating at 1.7375 GHz and 2.0375 GHz, with –10 dB impedance bandwidths of 72.5 MHz and 65.5 MHz, respectively. The return losses (S_{11}) were -15.2374 dB and -21.6264 dB.

The current distributions of the 1st iteration FACRDGPS are depicted in Fig. 12 and Fig. 13 at resonances of 1.7375 GHz and 2.0375 GHz, respectively.

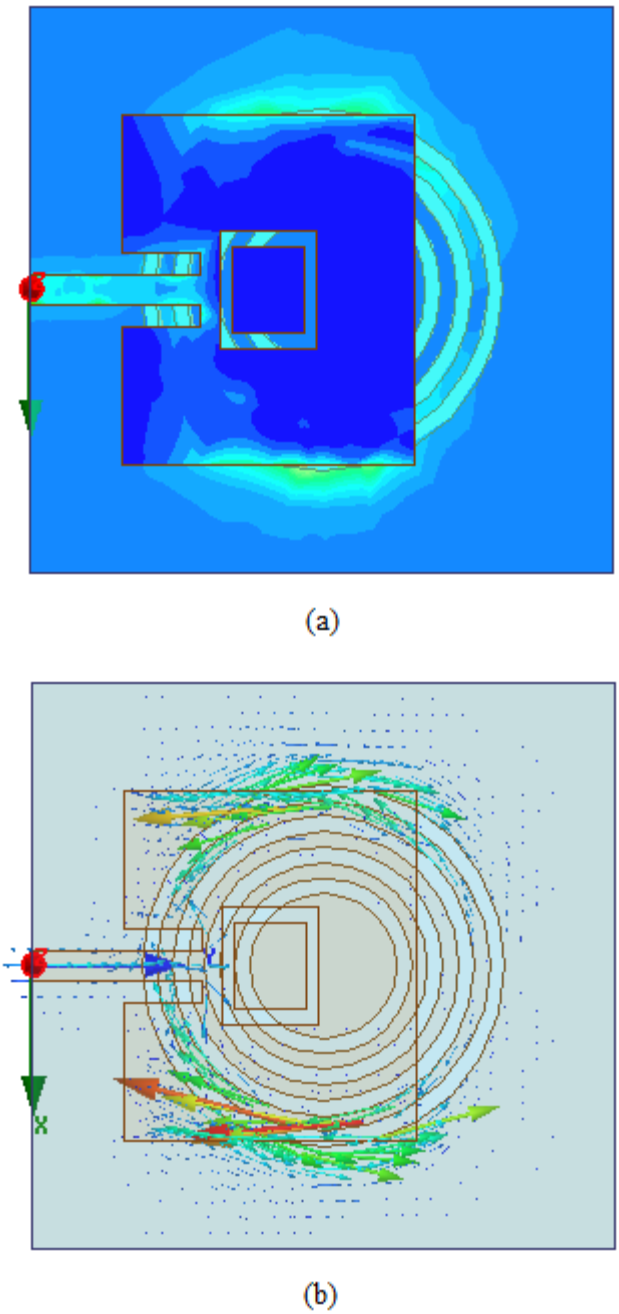

(a)

(b)

Fig. 12 Current distribution of the 1st iteration fractal antenna with concentric ring-shaped DGPS (FACRDGPS) at 1.7375 GHz; (a) Magnitude (b) Vector

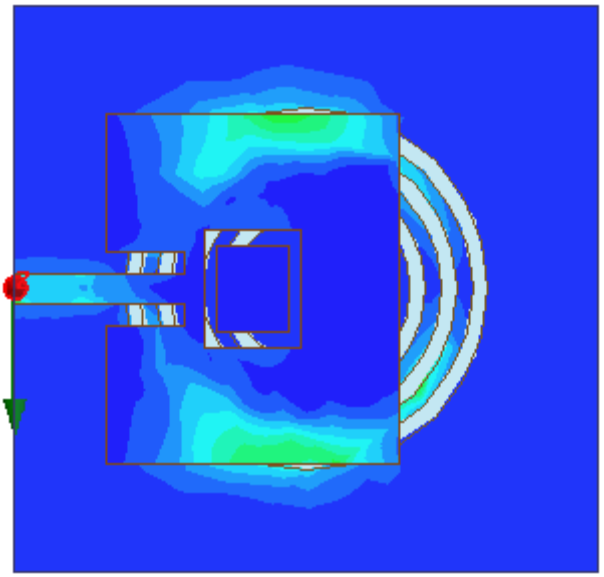

(a)

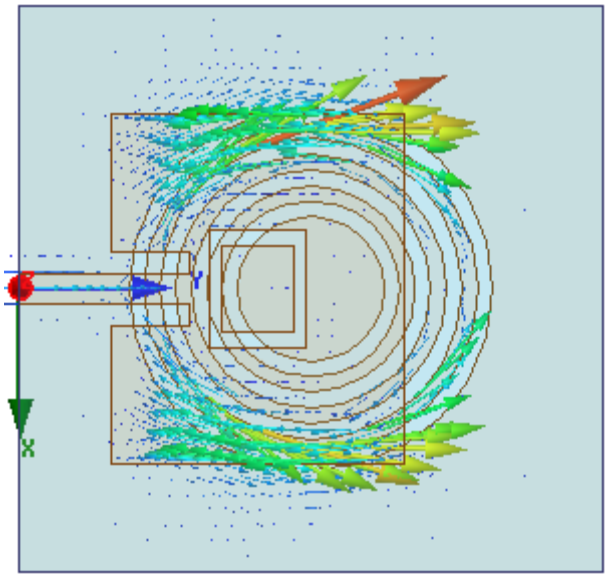

(b)

Fig. 13 Current distribution of the 1st iteration fractal antenna with concentric ring-shaped DGPS (FACRDGPS) at 2.0375 GHz; (a) Magnitude (b) Vector

From Fig. 12(b) and Fig. 13(b) for the 1st iteration FACRDGPS, compared to Fig. 9(b) of the conventional patch antenna, it can be observed that the disturbance of the current distribution caused by the excoriation of the fractals in the patch and the concentric ring-shaped defects in the ground plane causes the current to flow in two different paths. This leads to the dual-band resonance observed at 1.7375 GHz and 2.0375 GHz.

The radiation patterns of the 1st iteration FACRDGPS are plotted in Fig. 14 and Fig. 15, at 1.7375 GHz and 2.0375 GHz, respectively. From the current distribution plot (in vector form) of the 1st iteration FACRDGPS at 1.7375 GHz shown in Fig. 12(b), it is observed that current flows in the *y*-direction. Thus, the *yz*-plane is the *E*-plane whereas the *xz*-plane was the *H*-plane. The radiation pattern in the *E*-plane is observed to be bi-directional whereas that in the *H*-plane is observed to be omni-directional at 1.7375 GHz, as depicted in Fig. 14.

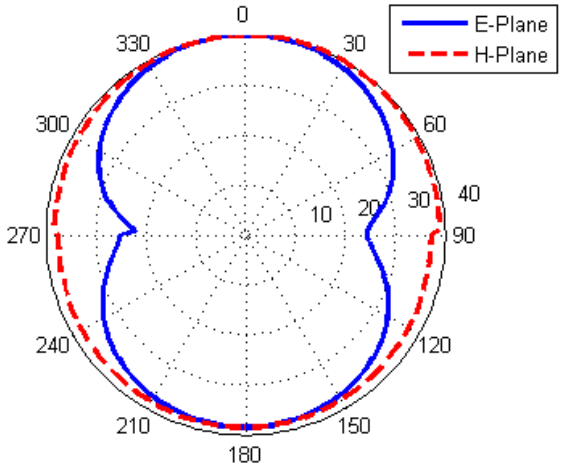

Fig. 14 Radiation pattern of the 1st iteration FACRDGPS at 1.7375 GHz

Similarly, from the current distribution plot (in vector form) of the 1st iteration FACRDGPS at 2.0375 GHz shown in Fig. 13(b), it is observed that current flows in the *y*-direction. Thus, the *yz*-plane is the *E*-plane whereas the *xz*-plane is the *H*-plane. The radiation pattern in the *E*-plane is observed to be bi-directional whereas that in the *H*-plane is observed to be omni-directional at 2.0375 GHz, as depicted in Fig. 15.

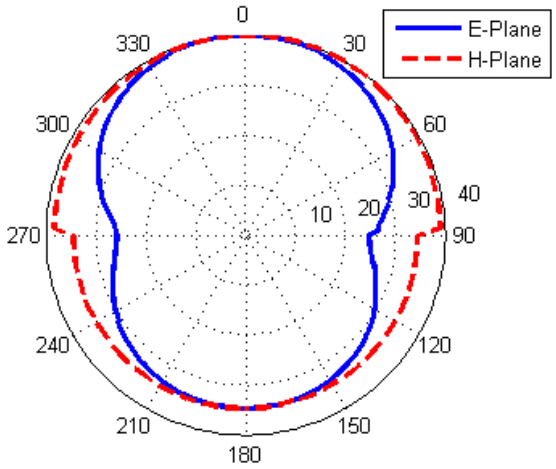

Fig. 15 Radiation pattern of the 1st iteration FACRDGPS at 2,0375 GHz

C. 2nd iteration FACRDGPS

The return loss plots of the 2nd iteration Fractal antenna with concentric ring-shaped DGPS (2nd iteration FACRDGPS) are shown in Fig. 16. The return loss plots of the Concentric Ring-shaped DGPSMA and fractal iteration 2 antenna are included for comparison.

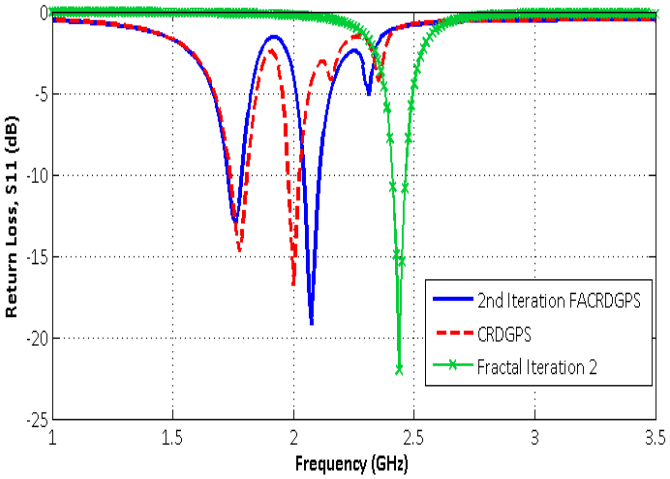

Fig. 16 Combined return loss plot of the 2nd iteration FACRDGPS, Concentric Ring-shaped DGPSMA and the 2nd iteration Fractal antenna

The 2nd iteration FACRDGPS exhibits dual-band resonance, with resonances at 1.7625 GHz and 2.0750 GHz, with –10 dB impedance bandwidths of 58.8 MHz and 66.8 MHz, respectively. The return losses (S_{11}) were -13.0195 dB and -19.2408 dB

The 2nd iteration FACRDGPS current distribution plots are shown in Fig. 17 and Fig. 18 at resonances of 1.7625 GHz and 2.075 GHz, respectively.

From Fig. 17(b) and Fig. 18(b) for the 2nd iteration FACRDGPS, compared to Fig. 9(b) for the conventional patch antenna, it can be observed that the disturbance of the current distribution caused by the excoriation of the fractals in the patch and the concentric ring-shaped defects in the ground plane causes the current to flow in two different paths. This leads to the dual-band resonance observed at 1.7625 GHz and 2.075 GHz.

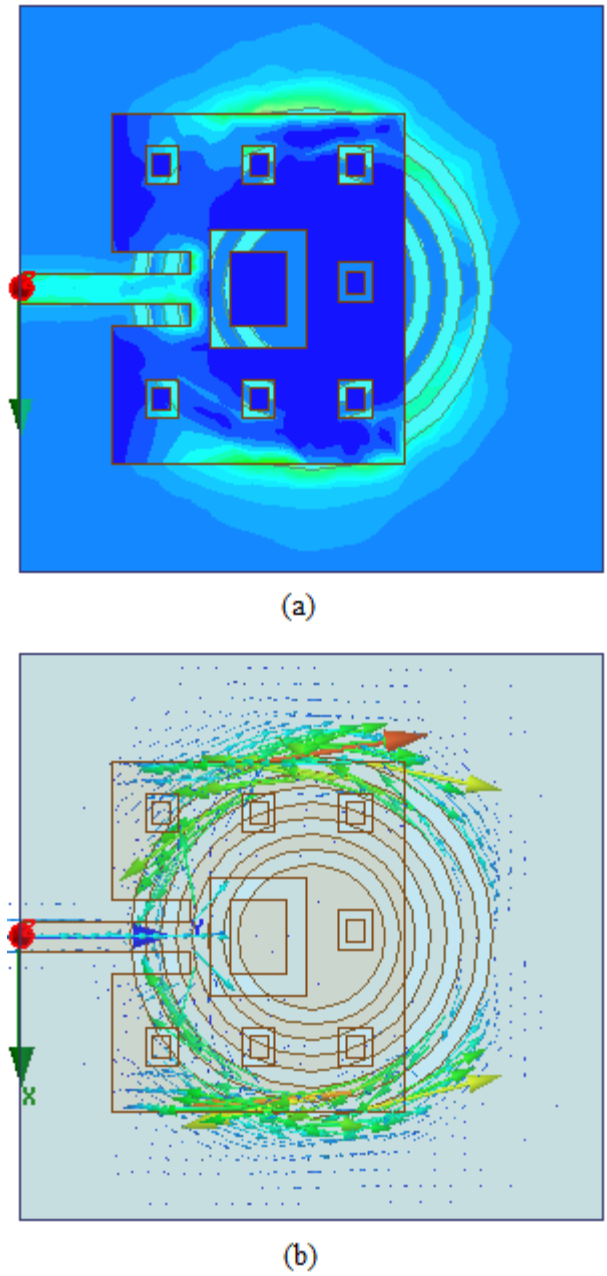

Fig. 17 Current distribution of the 2nd iteration fractal antenna with concentric ring-shaped DGPS (2nd iteration FACRDGPS) at 1.7625 GHz; (a) Magnitude (b) Vector

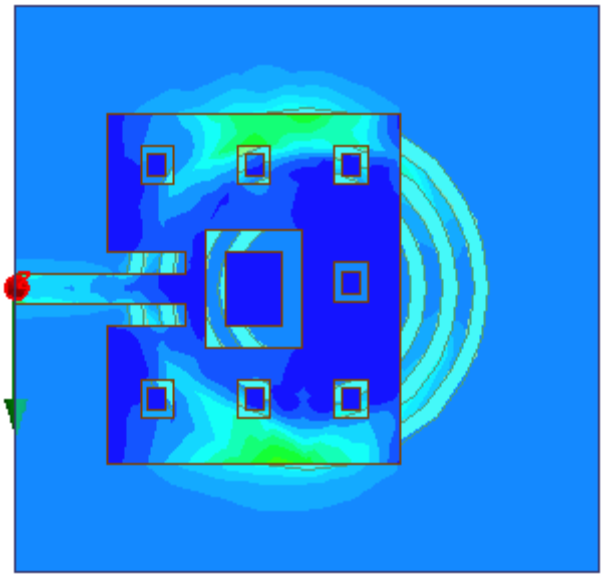

(a)

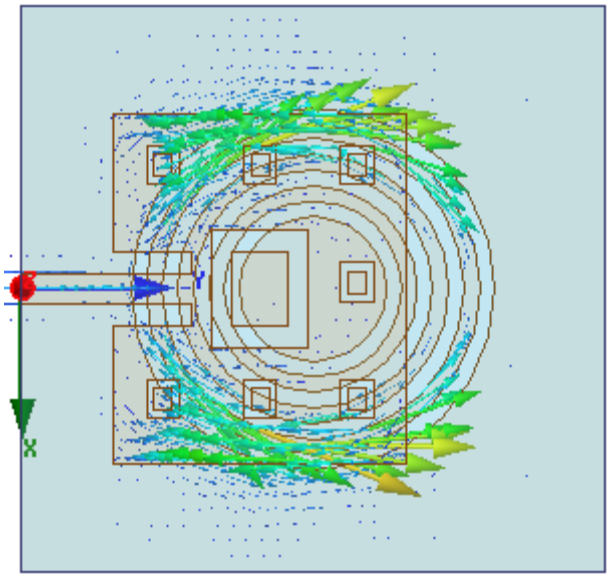

(b)

Fig. 18 Current distribution of the 2nd iteration fractal antenna with concentric ring-shaped DGPS (2nd iteration FACRDGPS) at 2.075 GHz; (a) Magnitude (b) Vector

The radiation patterns of the 2nd iteration FACRDGPS are plotted in Fig. 19 and Fig. 20, at 1.7625 GHz and 2.075 GHz, respectively. From the current distribution plot (in vector form) of the 2nd iteration FACRDGPS at 1.7625 GHz as shown in Fig. 17(b), it is observed that current flows in the *y*-direction. Thus, the *yz*-plane is the *E*-plane whereas the *xz*-plane was the *H*-plane. The radiation pattern in the *E*-plane is observed to be bi-directional whereas that in the *H*-plane is observed to be omni-directional at 1.7625 GHz, as depicted in Fig. 19.

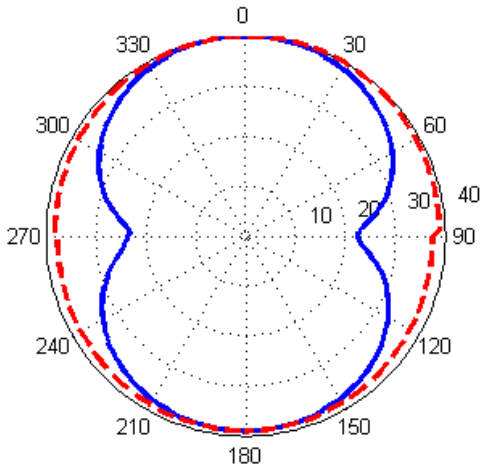

Fig. 19 Radiation pattern of the 2nd iteration FACRDGPS at 1.7625 GHz

Similarly, from the current distribution plot (in vector form) of the 2nd iteration FACRDGPS at 2.075 GHz shown in Fig. 18(b), it is observed that current flows in the *y*-direction. Thus, the *yz*-plane is the *E*-plane whereas the *xz*-plane was the *H*-plane. The radiation pattern in the *E*-plane was observed to be bi-directional whereas that in the *H*-plane was observed to be omni-directional at 2.075 GHz, as depicted in Fig. 20.

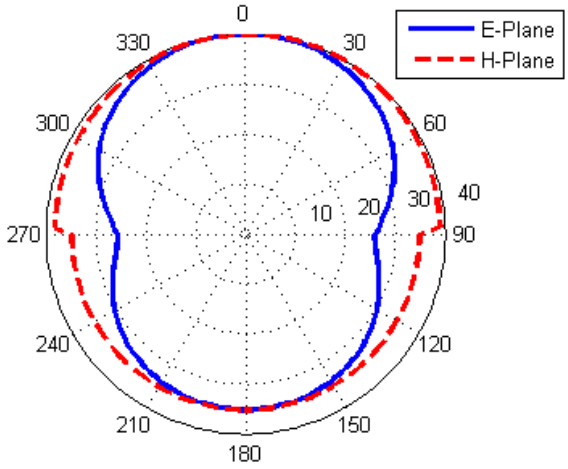

Fig. 20 Radiation pattern of the 2nd iteration FACRDGPS at 2.075 GHz

Fig. 21 shows a combined VSWR plot of the 1st and 2nd iterations of the FACRDGPS. For the 1st iteration, the VSWR is < 2 for the frequencies 1.7011-1.7785 GHz for the lower resonance band and 2.0054-2.0733 GHz for the upper resonance band. For the 2nd iteration, the VSWR is < 2 for the frequencies 1.7235-1.7885 GHz for the lower resonance band and 2.0399-2.1097 GHz for the upper resonance band.

The VSWR being < 2 in these resonance bands indicates good impedance matching.

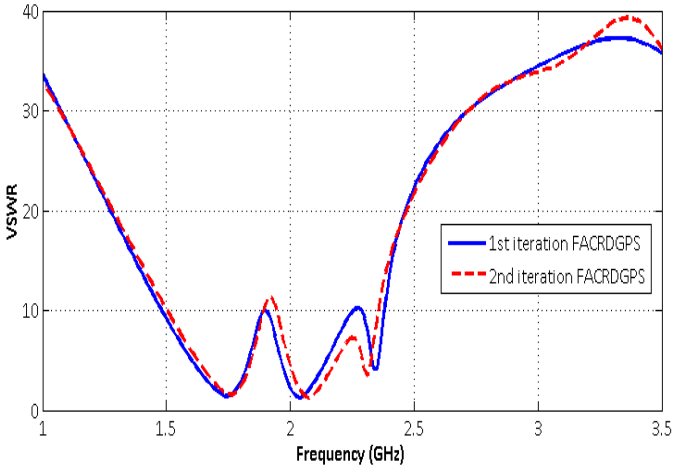

Fig. 21 Combined VSWR plot of the 1st and 2nd iteration FACRDGPS

Thus in summary, from Fig. 11 and Fig. 16, for the 1st and 2nd iteration FACRDGPPS, respectively, it can be observed that incorporating defected ground plane structure in addition to the fractals in the patch in an antenna leads to dual-band performance for both iterations, when compared to the antenna in [20], which only incorporates fractals in the patch and has single band resonance.

D. FABRICATION AND EXPERIMENTAL RESULTS

The 1st iteration Fractal antenna with Concentric Ring-shaped DGPS (FACRDGPS) is fabricated. The 1st iteration FACRDGPS is chosen for fabrication since it exhibits dual-band resonance with larger bandwidth and matching (with regard to lower return loss) when compared to the 2nd iteration FACRDGPS.

Fig. 22 shows images of the fabricated 1st iteration FACRDGPS. The fabrication is undertaken on a pre-sensitized double-sided printed circuit board made of FR4 epoxy substrate with a thickness h=1.6 mm and dielectric constant $\varepsilon_r = 4.7$.

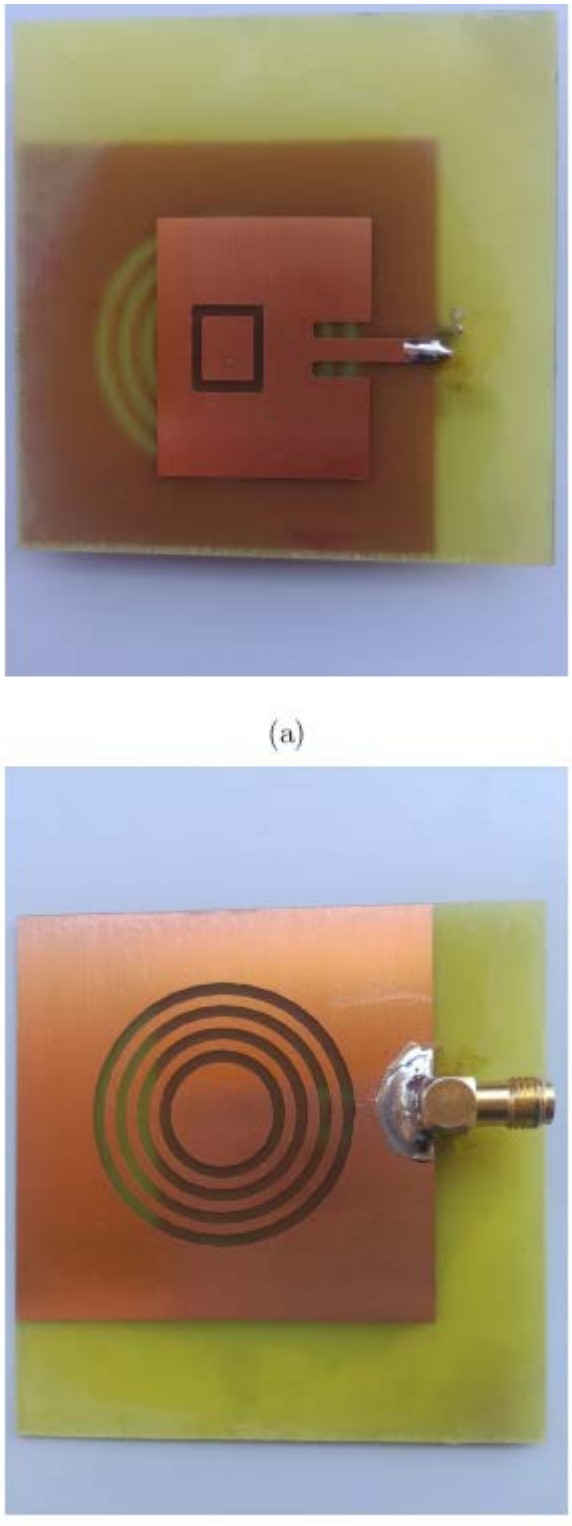

Fig. 22 Images of the fabricated 1st iteration Fractal antenna with Concentric Ring-shaped DGPS (FACRDGPS) (a) Patch (b) Ground plane

The fabricated patch antenna is tested in the laboratory using an MS2027C Anritsu Vector Network Analyzer (VNA) master. Before the return loss measurements are taken, the Anritsu VNA is calibrated for accurate measurement. Since only one

port is used for the return loss (S_{11}) measurement, only Port 1 of the Vector Network Analyzer is calibrated.

The experimental setup is shown in Fig. 23.

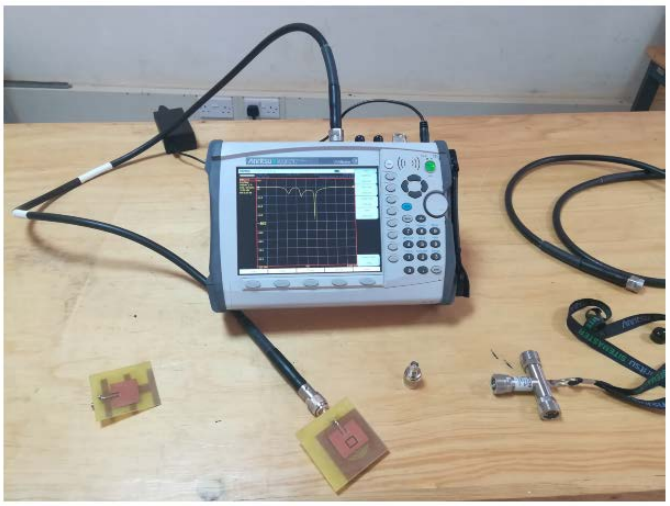

Fig. 23 The experimental set up used for the return loss measurement using the MS2027C Anritsu Vector Network Analyzer

Fig. 24 compares the simulated and the measured return loss plots of the 1st iteration Fractal antenna with Concentric Ring-shaped DGPS (1st iteration FACRDGPS).

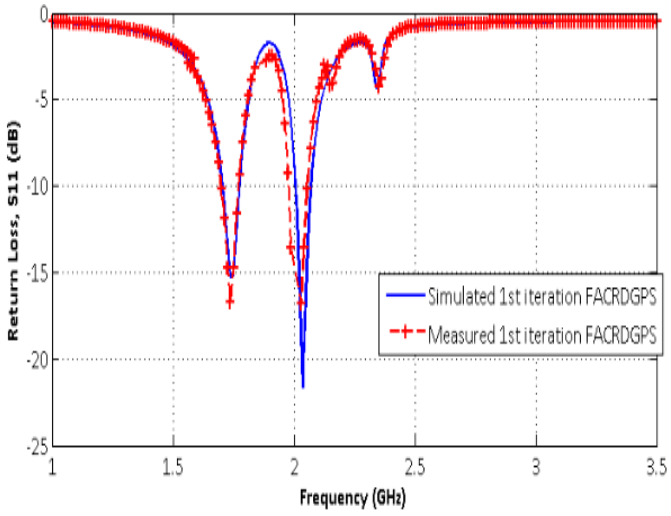

From Fig. 24, the fabricated 1st iteration Fractal antenna with Concentric Ring-shaped DGPS (FACRDGPS) exhibits dual-band resonances at 1.74 MHz and 2.03 MHz, with bandwidths of 73.4 MHz and 67.6 MHz, respectively, compared to the simulated bandwidths of 72.5 MHz and 65.5 MHz. Thus there is good agreement between the simulated and the measured return loss. The slight shift in the resonance frequencies can be attributed to tolerance in the fabrication process.

IV. Conclusion

In this paper, dual-band antennas have been designed by combining the fractal design technique on the patch and the defected ground plane structure in the ground plane in an inset fed micro-strip antenna. The fractal design technique only produces a single band of resonance. By incorporating concentric ring-shaped defected ground structures in the ground plane of the same fractal antenna, better antennas with dual-band resonance are designed.

The designed antennas also exhibit low return losses which indicate good impedance matching. For all antennas, the VSWR is also < 2, which also indicates good matching.

The measured return loss of the 1st iteration FACRDGPS also compared well with the simulated return loss.

The designed antennas can be used for mobile communication, and satellite radio applications since the resonance frequencies are located in UHF band.

References

[1] C. A. Balanis, "Microstrip antennas," in *Antenna Theory: Analysis and Design*. New Jersey, United States of America: John Wiley and Sons, 2005, ch. 14, pp. 811-872.

[2] S. Jaiswal, A. Kumar, and N. Kumari, "Development of Wireless Communication Networks: From 1G to 5G," *International Journal of Engineering and Computer Science*, vol. 3, no. 5, pp. 6053-6056, May 2014.

[3] L. Cheema and K. K. Sherdia, "Design of Microstrip Antenna with Defected Ground Structure for UWB Applications," *International Journal of Advanced Research in Computer and Communication Engineering*, vol. 2, no. 7, pp. 2525-2528, July 2013.

[4] H. Elftouh et al., "Miniaturized microstrip patch antenna with defected ground structure," *Progress In Electromagnetics Research C*, vol. 55, pp. 25-33, 2014.

[5] T. Wang, Y. -Z. Yin, J. Yang, Y. -L. Zhang, and J. -J. Xie, "Compact Triple-Band Antenna using Defected Ground Structure for WLAN/WIMAX Applications," *Progress in Electromagnetics Research Letters*, vol. 35, pp. 155-164, 2012.

[6] R. Saini and D. Parkash, "Design and Simulation of CPW Fed Slotted Circular Microstrip Antenna with DGS for Wireless Applications," *International Journal of Applied Sciences and Engineering Research*, vol. 3, no. 1, pp. 82-90, 2014.

[7] G. Singh and A. Marwaha, "Design of G-shaped Defected Ground Structure for Bandwidth Enhancement," *International Journal of Computer Applications*, vol. 75, no. 9, pp. 7-11, Aug. 2013.

[8] R. Mudgal and L. Shrivastava, "Microstrip V-slot Patch Antenna using an H-slot Defected Ground Structure," *International Journal of Technology Enhancements and Emerging Engineering*, vol. 2, no. 2, pp. 21-24, 2014.

[9] N. A. Khan and B. A. Singh, "Microstrip Antenna Design with Defected Ground Structure," *IOSR Journal of Electronics and Communication Engineering (IOSR-JECE)*, vol. 9, no. 2, pp. 46-50, March 2014.

[10] C. A. Balanis, "Frequency Independent Antennas, Antenna Miniaturization and Fractal Antennas," in *Antenna Theory: Analysis and Design*. New Jersey: John Wiley and Sons, 2005, pp. 611-652.

[11] H. Zang, X. Zhao, X. Xu, G. Zhang, and J. Lu, "A Review of Fractal Antennas," *International Journal of Future Computing and Communication Engineering*, pp. 15-18, 2014.

[12] F. Viani, "Dual-Band Sierpinski Pre-Fractal Antenna for 2.4 GHz WLAN and 800 MHz LTE Wireless Devices," *Progress in Electromagnetics Research C*, vol. 35, pp. 63-71, 2013.

[13] A. Aggarwal and M. V. Kartikeyan, "Pythagoras tree: A fractal patch antenna for multi frequency and ultra-wide bandwidth operations," *Progress In Electromagnetics Research C*, vol. 16, pp. 25-35, 2010.

[14] S. Chauhan, J. K. Deegwal, D. Soni, and P. Singondia, "A Design of Crown-Shape Fractal Patch Antenna," *International Journal of Engineering and Innovative Technology*, vol. 2, no. 3, pp. 177-179, Sep. 2010.

[15] V. Ram, V. Anjaria, P. Boriya, and N. Patel, "Design and Development of Switchable Fractal Patch Antenna for GPS Application," *International Journal of Engineering Science*, vol. 1, no. 7, pp. 46-50, Nov. 2012.

[16] N. Bisht and P. Kumar, "A Dual Band Fractal Circular Microstrip Patch Antenna for C-Band Application," in *Progress in Electromagnetics Research Symposium Proceedings*, Suzhou, China, 2011, pp. 852-855.

[17] M. Susila, T. Rao, and A. Gupta, "A novel smiley fractal antenna (SFA) design and development for ulra-wideband wireless applications," *Progress In Electromagnetics Research C*, vol. 55, pp. 25-33, 2014.

[18] N. Chaudhary, S. Sindhiya, and K. K. TirPhati, "Design and analysis of multiband slotted octagonal fractal antenna," *International Journal of Advanced Research in electronics and Communication Engineering*, vol. 3, no. 1, pp. 41-46, January 2014.

[19] N. Trivedi, S. Gurjar, and A. K. Singh, "Design and Simulation of Novel I Shape Fractal Antenna," *International Journal of Engineering Science and Technology*, vol. 4, no. 11, pp. 4669-4675, Nov. 2012.

[20] S. Shrestha et al., "Design of modified Sierpinski fractal based miniaturized patch antenna," *ICOIN*, pp. 274-279, 2013.

[21] C. A. Balanis, "Microstrip antennas: Feeding methods," in *Antenna Theory: Analysis and Design*. New Jersey, United States of America: John Wiley and Sons, 2005, ch. 14, pp. 813-815.

[22] S. B. Patil, R. D. Kanphade, and V. V. Ratnaparkhi, "Design and Performance Analysis of Inset fed Microstrip Square Patch Antenna for 2.4 GHz Wireless Applications," *IEEE Sponsored 2nd International Conference on Electronics and Communication Systems (ECECS 2015)*, pp. 1194-1200, 2015.